Universiteit
Leiden
The Netherlands

Squaramide-based supramolecular materials for 3D cell culture applications

Tong, C.

Citation
Tong, C. (2021, March 10). *Squaramide-based supramolecular materials for 3D cell culture applications*. Retrieved from https://hdl.handle.net/1887/3151624

Version:	Publisher's Version
License:	Licence agreement concerning inclusion of doctoral thesis in the Institutional Repository of the University of Leiden
Downloaded from:	https://hdl.handle.net/1887/3151624

Note: To cite this publication please use the final published version (if applicable).

Cover Page

Universiteit Leiden

The handle https://hdl.handle.net/1887/3151624 holds various files of this Leiden University dissertation.

Author: Tong, C.
Title: Squaramide-based supramolecular materials for 3D cell culture applications
Issue Date: 2021-03-10

CHAPTER 5

Photo-activatable double networks based on one-dimensional supramolecular and covalent polymers for 3D chondrocyte culture

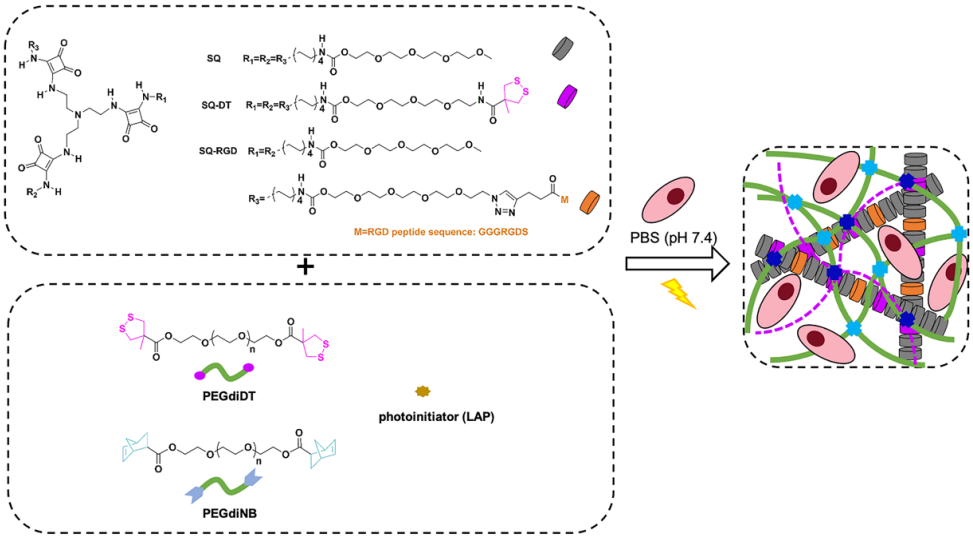

This chapter was prepared as an original research paper: Ciqing Tong, Joeri A. J. Wondergem, Doris Heinrich, Yolande F. M. Ramos, and Roxanne E. Kieltyka

5.1 Abstract

Hybrid supramolecular and covalent double network (DN) hydrogels are highly suitable for applications in 3D platforms for articular cartilage engineering because of their mechanical properties and structural features that are comparable to the *in vivo* extracellular matrix (ECM). Herein, we explore the use of photoactive cyclic 1,2-dithiolanes (DT) to prepare double network materials through the crosslinking of one-dimensional supramolecular and covalent polymeric networks. Two-photon patterning and oscillatory rheology studies demonstrate that mechanical, self-recovery and compressive properties of the DN hydrogels can be easily modulated with spatiotemporal control using light and by varying the compositional parameters of the supramolecular/polymer mixture, allowing spatial and temporal control over the hydrogel stiffness and introduction of bioactive cues. 3D encapsulation of NIH 3T3 fibroblasts and human primary articular chondrocytes (hPACs) with different UV light exposure times was achieved with high cell viability. ECM deposition during 3D culture of hPACs was visualized showing increased levels of sulphated-glycosaminoglycans (s-GAGs) with increasing stiffness of the DN hydrogels. Taken together, hybrid supramolecular and covalent DN hydrogels show promise as synthetic scaffolds for applications involving articular cartilage.

5.2 Introduction

Hydrogels based 3D scaffolds for tissue engineering of cartilage are an effective repair strategy to address the poor healing and regenerative ability of articular cartilage *in vivo*.[1-6] In order to prepare the ideal matrix for chondrocyte culture, the designed hydrogels should favor their survival without affecting their regular behaviour (e.g., ECM production and deposition).[2,3] In the joint, the interactions between the proteoglycans and fibrous collagen II enable the ECM to resist the mechanical loading from cartilage.[2,3,7] Therefore, hydrogels with high mechanical stiffness and strength are required for use in cartilage tissue engineering.[4] However, in general, traditional synthetic hydrogels composed of single networks either of supramolecular or covalent polymers are typically brittle and fragile in character.[8]

Double network (DN) hydrogels consisting of two independent networks and dual crosslinked junctions formed through physical or chemical interactions demonstrate improved mechanical strength and stiffness overcoming the limitations of single synthetic networks.[8-10] In the field of cartilage tissue engineering these materials have attracted much attention because of their capacity to mimic the properties of load bearing tissues, such as cartilage, bone, ligaments and tendons.[11,12] However, it remains challenging to prepare synthetic networks that have the necessary compressive and tensile strengths, while maintaining the various criteria that are necessary for 3D cell culture and tissue engineerings such as facile sample preparation strategy, cytocompatibility, and multiple biological cues (e.g., cell degradation, adhesion).[11]

More recently, supramolecular and covalent polymer-based DN hydrogels have been developed that use supramolecular chemistry to provide outstanding properties such as self-healing and energy dissipation during mechanical loading, that are not accessible in most conventional fully covalent polymer-based DN hydrogels.[11,13-22] For example, supramolecular hydrogels based stacked monomers or polymers with molecular recognition units have been used for crosslinking and engineering of the cell microenvironment in 3D.[14-16,21-23] In particular, incorporating supramolecular networks based on 3D entangled fibers enable the resultant DN hydrogels to more closely mimic the fibrous structure of native proteins such as collagen found in articular cartilage.[2,3] Thus far, most studies have explored peptide-based hydrogels to fabricate to prepare such DN hydrogels for tissue engineering applications,[16,17] but very few examples have reported the use of low molecular weight hydrogels. Using such an approach is would be

advantageous because of its economic nature to facilitate bioink development for 3D bioprinting and cell delivery.[5]

In this study, we explore a facile strategy to prepare photoactive supramolecular and covalent polymer-based DN hydrogels that combine one-dimensional squaramide-based supramolecular polymers and covalent polymers (**Figure 5.1**). Light activatable, 1,2-dithiolanes (DT)[24-27] were tethered to both polymers to facilitate their photo-crosslinking using UV light in the range of 365-375 nm. We specifically investigated the mechanical and biological properties of obtained supramolecular and covalent polymer DN hydrogels as a function of modulating their hydrogel compositions. The cytocompatibility of the DN hydrogel matrices for 3D cell culture of several cell types including human articular chondrocytes (hPACs) was also examined. The matrix deposition by encapsulated hPACs cells indicates their potential application for cartilage regeneration.

5.3 Results and discussion

5.3.1 Design of the supramolecular and covalent polymer-based hybrid hydrogels

To engineer a novel hybrid hydrogel with high strength and stiffness, supramolecular and covalent polymer based cross-linked network architectures were explored. As described in **chapter 3**, the multicomponent based supramolecular hydrogels (SG), namely, **SQxSQ-DTySQ-RGD** (x, y: molar percent of **SQ-DT** and **SQ-RGD** co-assembled with **SQ**) were formed through the entanglements and their stiffness was modulated through the light activated cross-linking between the tripodal squaramide based monomers by virtue of 1,2-dithiolane moiety. The mechanical and cell-adhesive properties of these hydrogels were easily controlled by independently varying the introduced concentration of the **SQ-DT** and **SQ-RGD** during the self-assembly process. On the other hand, the PEG-based polymeric hydrogels (PG) from **chapter 4**, specifically, $\mathbf{PEG_{m\text{-}n}}$ (m and n: the architecture of dithiolane (DT) and norbornene (NB)-functionalized PEG polymers), were shown to be covalently crosslinked through the photo-induced one-pot DT-NB reaction.[26] Hence, we combined these two networks to prepare DN hydrogels (**Figure 5.1A**) using **SQ-DT** to trigger the formation of reversible covalent cross-links due to the ring-opening polymerization of DT with the DT/NB groups from the covalent PEG polymers in one-pot using UV light irradiation. Besides, the interpenetrating polymer network (IPN) that does not have the

supramolecular and covalent network connected through covalent crosslinks was also studied as a control.

In this study, a simple three-step strategy was used to prepare the supramolecular and covalent DN hydrogels (**Figure 5.1B**). Firstly, to achieve a homogeneous supramolecular and covalent polymer solution, a supramolecular network stock solution (**SQxSQ-DTySQ-RGD**) was sonicated in an ice bath and then the covalent polymer stock solution (e.g., **$PEG_{2\text{-}2}$**), containing the photoinitiator lithium phenyl-2,4,6-trimethylbenzoylphosphinate (**LAP**), was directly added by gently pipetting up and down (10 times) prior to gel formation. During the mixing process, the volume ratio of the supramolecular to covalent polymer solution was maintained at a ratio of 4:1. Secondly, the obtained supramolecular and covalent polymer mixtures were equilibrated at 37 ^{o}C for 15 min to trigger supramolecular hydrogel formation and were stored at room temperature overnight. Finally, UV light (1-10 min, ~10 mW/cm^2, 365-375 nm) was applied to trigger the formation of hybrid DN hydrogels. This photoirradiation step simultaneously initiates additional chemical cross-linking between the two networks in one-pot. Various parameters such as the total supramolecular monomer concentration, the molar percentage of **SQ-DT** in the supramolecular mixture, the total polymer concentration and the architecture dependence of the DT/NB functionalized PEG precursors **$PEG_{m\text{-}n}$** (e.g., m-n: 2-2; 2-4; 4-4) were examined to tune the properties of hybrid DN hydrogels. All the hydrogels were prepared following the described three-step general procedure.

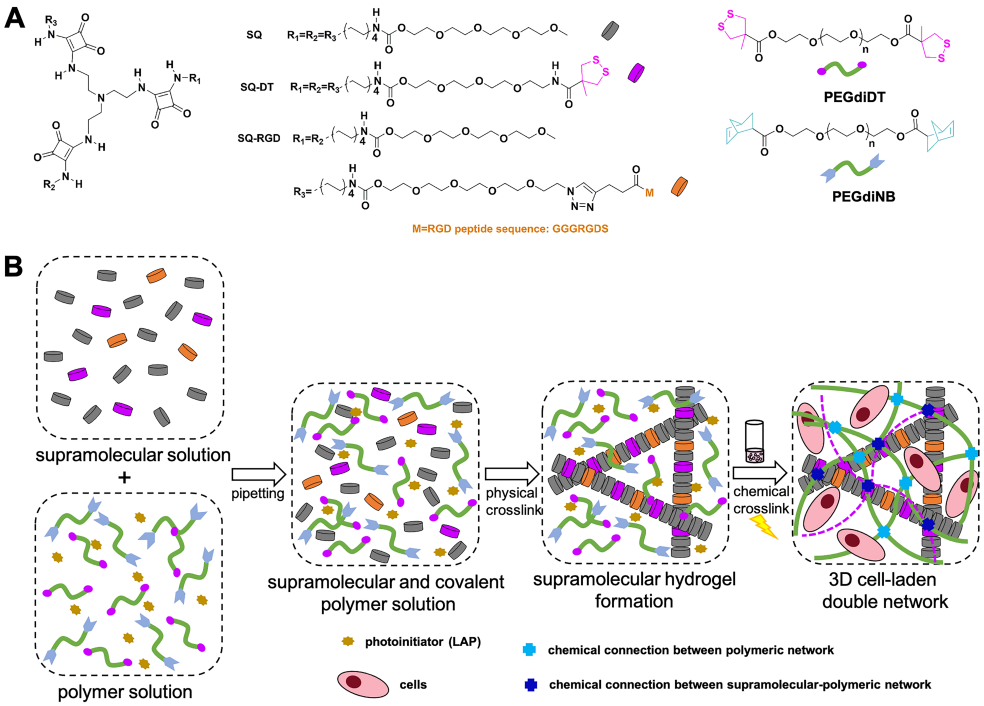

Figure 5.1 (A) Chemical structure of squaramide based supramolecular monomers (**SQ**, **SQ-DT** and **SQ-RGD**) and PEG-based polymeric monomers (**PEGdiDT** and **PEGdiNB**); (B) Schematic illustration for the preparation of 3D cell-laden supramolecular and covalent polymer based double networks, which follow three general steps and use UV irradiation (1-10 min, ~10 mW/cm^2, 365-375 nm) to initiate covalent bond formation.

5.3.2 Characterization of hydrogels

To better understand the mechanical properties of the various supramolecular and covalent DN hydrogels prepared, oscillatory rheology measurements were performed. As shown in the gel inversion experiment (**Figure S5.1**), transparent hydrogels were obtained after UV irradiation using a benchtop LED source (3 min, ~10 mW/cm^2, 375 nm). In the first step, the mechanical properties of the single network (SG and PG) and double network were examined. After 10 min UV irradiation (~10 mW/cm^2, λ = 320-500 nm, primary peak: 365 nm), the storage modulus (G') for polymeric hydrogel **PEG$_{2\text{-}2}$** (6.0 mM) containing **PEGdiDT** (3.0 mM) and **PEGdiNB** (3.0 mM) with **LAP** (1.0 mM) was 1284 ± 56 Pa, and the G' of the supramolecular hydrogel containing **SQ10SQ-DT** (5.0 mM) was 2816 ± 519 Pa (**Figure 5.2A**). When the above two systems were combined under identical UV exposure conditions, the obtained DN hydrogel (5.0 mM **SQ10SQ-DT**/6.0 mM **PEG$_{2\text{-}2}$**) exhibited a high storage modulus (G' = 10391 ± 541 Pa), which is

mechanically stronger by one order of magnitude than the sum of the SG and PG gels separately highlighting the synergy of mixing these two networks on the mechanical properties. Moreover, the gelation time was reduced (~3 min) when compared to the SG hydrogel (~10 min), as evidenced by the rapid achievement of the maximum G' within the time sweep curve (**Figure 5.2A**). Further rheological experiments revealed that the monomer **SQ-DT** and the other three components **PEGdiDT**, **PEGdiNB** and **LAP**, were required to achieve a DN hydrogel with the highest storage modulus (5.0 mM **SQ10SQ-DT**/6.0 mM **$PEG_{2\text{-}2}$**). The absence of either of these components was found to lower the storage modulus to 234 ± 11 Pa (**Figures 5.2B** and **S5.3**).

The mechanical properties of the various DN hydrogels (**SQxSQ-DT/$PEG_{m\text{-}n}$**) were further modulated by controlling several parameters, for example, the molar percentage (x) of **SQ-DT** in **SQxSQ-DT**, the total supramolecular concentration of **SQxSQ-DT**, the total polymer concentration of **$PEG_{m\text{-}n}$**, the **$PEG_{m\text{-}n}$** polymer architecture and the UV light source (**Table S5.1**). These results demonstrate that in hydrogels containing 5.0 mM **SQxSQ-DT**/6.0 mM **$PEG_{2\text{-}2}$**, increasing the molar percentage (x) of **SQ-DT** from 0% to 10% results in an increased G' (from 4193 Pa to 10391 ± 541 Pa) that reaches saturation at 10% (**Figure 5.2C**). By further increasing the total supramolecular concentration, while maintaining the same overall concentration of both the **SQ-DT** and polymer concentrations, the final storage modulus of the DN hydrogel (10.0 mM **SQ5SQ-DT**/6.0 mM **$PEG_{2\text{-}2}$**) was comparable to the DN hydrogel (5.0 mM **SQ10SQ-DT**/6.0 mM **$PEG_{2\text{-}2}$**) (**Figure S5.4**). Furthermore, a wide range of hydrogel stiffnesses, from 3028 ± 129 Pa to 21072 ± 5071 Pa, was obtained by tuning the total **$PEG_{2\text{-}2}$** polymer concentration from 3.0 mM to 16.0 mM in 5.0 mM **SQ10SQ-DT/$PEG_{2\text{-}2}$** hydrogel (**Figure 5.2D**). In contrast, mixing higher concentrations of the **$PEG_{2\text{-}2}$** network (e.g., 12.0 mM and 16.0 mM) only resulted in a slight improvement of G' of the DN hydrogel. It is likely due to the formation of viscous solution at higher covalent polymer concentrations instead of weak gel for supramolecular and covalent polymer mixtures prior to UV irradiation as shown in rheological measurements (**Table S5.1**). When SG hydrogel (5.0 mM **SQ10SQ-DT**) was mixed with the different polymer architectures of **$PEG_{m\text{-}n}$** with the equal molar concentration of the DT and NB active motifs, for example, from linear architecture (6.0 mM **$PEG_{2\text{-}2}$**) to the multi-architecture (e.g., 4.5 mM **$PEG_{2\text{-}4}$** and 3.0 mM **$PEG_{4\text{-}4}$**), all DN hydrogels demonstrated comparable G' values pointing to the incorporation of the PG with similar crosslinking density (**Figure 5.2E**). Finally, the G' of the DN hydrogel (5.0 mM **SQ10SQ-DT**/6.0 mM

PEG$_{2\text{-}2}$) was modulated in a stepwise manner by switching the light source on and off at various time points, showing the capacity to modulate spatial- and temporal properties of the hydrogel (**Figure S5.5**).

The self-recovery property of the DN hydrogels due to the combination of the supramolecular and reversible covalent cross-links provided by the disulfide bonds formed between both networks was also studied. Their combined effect was characterized by oscillatory rheology through a step-strain experiment. For example, the DN hydrogel (5.0 mM **SQ10SQ-DT**/6.0 mM **PEG$_{2\text{-}2}$**) showed in inversion in G' and G" after the application of high strain (500%) (**Figure 5.2F**). Subsequently, when a lower strain (0.05%) was applied, the hydrogel recovered 51% of its original G' within 5 min. Similar results were obtained when applying alternating low (0.05%) and high strains (500%) for two cycles. Interestingly, the recovery rate could be improved from 11% to 64% by tuning the total polymer concentration and also the polymer architecture in the DN hydrogels (**Figure S5.6**).

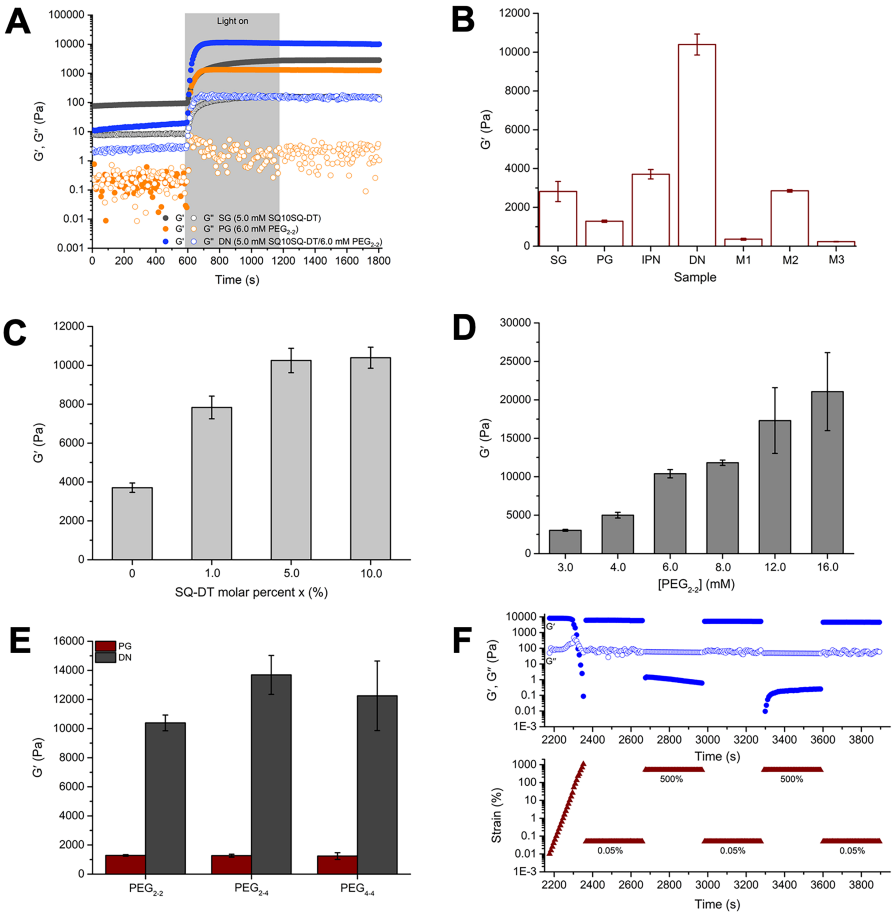

Figure 5.2 Oscillatory rheology data of hybrid DN gels: (A) Averaged (N = 3) time sweep of hydrogel systems (SG, PG and DN) through 10 min UV irradiation at room temperature using a fixed strain (γ = 0.05%) and frequency (f = 1.0 Hz). The shaded region indicates when the UV light irradiation was applied. (B) The plateau storage moduli (G') of various hydrogels after 10 min UV irradiation: SG (5.0 mM **SQ10SQ-DT**); PG (6.0 mM **PEG$_{2\text{-}2}$**); IPN (5.0 mM **SQ0SQ-DT**/6.0 mM **PEG$_{2\text{-}2}$**); DN (5.0 mM **SQ10SQ-DT**/6.0 mM **PEG$_{2\text{-}2}$**); M1 (5.0 mM **SQ10SQ-DT**/6.0 mM **PEG$_{2\text{-}2}$**/no **LAP**); M2 (5.0 mM **SQ10SQ-DT**/3.0 mM **PEGdiNB**/1.0 mM **LAP**); and M3 (5.0 mM **SQ10SQ-DT**/3.0 mM **PEGdiDT**/1.0 mM **LAP**). (C) The plateau G' of hydrogels (5.0 mM **SQxSQ-DT**/6.0 mM **PEG$_{2\text{-}2}$**) with various molar percent (x) of **SQ-DT** within the supramolecular hydrogel (5.0 mM **SQxSQ-DT**) after 10 min UV irradiation. (D) The plateau G' of DN hydrogel (5.0 mM **SQ10SQ-DT**/**PEG$_{2\text{-}2}$**) with varied total polymer concentrations (from 3.0 mM to 16.0 mM) after 10 min UV irradiation. (E) The plateau G' of PG and DN hydrogel containing varied polymer architectures (e.g., 6.0 mM **PEG$_{2\text{-}2}$**, 4.5 mM **PEG$_{2\text{-}4}$** and 3.0 mM **PEG$_{4\text{-}4}$**) with the same concentration of DT and NB motifs after 10 min UV irradiation. (F) Averaged (N = 3) strain experiment and step-strain measurement of DN hydrogel (5.0 mM **SQ10SQ-DT**/6.0 mM **PEG$_{2\text{-}2}$**) after 10 min UV light irradiation at a constant of frequency (f = 1.0 Hz). For all measurements, UV light irradiation condition: ~10 mW/cm^2, wavelength: 320-500 nm, primary peak: 365 nm. The average of several independent measurements (N = 3) was used to set the error bars.

The force-compression (normal stress-cauchy strain) curves of various hydrogels after 10 min UV light irradiation were obtained using the axial force compression test in the rheometer. The SG hydrogel (5.0 mM **SQ10SQ-DT**) was brittle and could only be compressed to 0.6% (μm/μm) of its original height with low fracture stress of 0.47 Pa (**Figure 5.3**). Notably, due to the relatively stable chemical crosslinks of DT and NB moieties, the PG hydrogel (e.g., 6.0 mM **$PEG_{2\text{-}2}$**) could endure up to 12% compression with increased fracture stress of 85 kPa. Moreover, the compression properties for PG hydrogels could be tuned by varying the total PEG polymer concentration and also the polymer architecture (**Figure S5.8**). Using the **$PEG_{2\text{-}2}$** hydrogel as an example, the higher polymer concentration (12.0 mM) required a higher normal stress (232 kPa) to be applied to fracture the hydrogel as compared to systems with a low polymer concentration (4.0 mM) that fractured at a stress of 35 kPa. However, the compressibility was sharply reduced from 20% to 7% of its initial height with the increase of total polymer concentration from 4.0 mM to 12.0 mM. Changing the polymer architecture from **$PEG_{2\text{-}2}$** to **$PEG_{4\text{-}4}$** and maintaining a comparable hydrogel stiffness, only showed a slight decrease in compression height and fracture stress of the materials (**Figure S5.8**). When the PG was added to the SG, all the IPN and DN hydrogels showed a decrease in compressibility. However, the normal stress in the fracture of the DN hydrogel was increased to 178 kPa (5.0 mM **SQ10SQ-DT**/4.5 mM **$PEG_{2\text{-}4}$**). In comparison, there was no significant difference in the fracture stress between theIPN (5.0 mM **SQ0SQ-DT**/6.0 mM **$PEG_{2\text{-}2}$**) and PG (6.0 mM **$PEG_{2\text{-}2}$**) systems, which may due to the absence of covalent cross-links between the two networks (**Figure 5.3**).

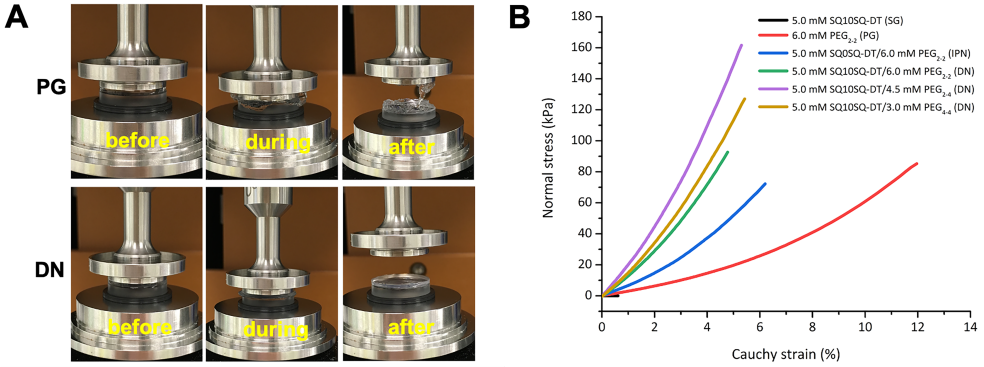

Figure 5.3 (A) Optical images illustrating the different states of hydrogels PG (6.0 mM **PEG$_{2\text{-}2}$**) and DN (5.0 mM **SQ10SQ-DT**/6.0 mM **PEG$_{2\text{-}2}$**) after 10 min UV irradiation (~10 mW/cm^2, wavelength: 320-500 nm, primary peak: 365 nm) before/during/after the force experiments using rheology. (B) The averaged (N = 3) normal stress-cauchy strain curves of different hydrogel samples (SG, PG, IPN and DN).

Scanning electron microscopy (SEM) was used to provide insight into the microscopic structure of the gels and to further compare their mechanical properties. As shown in **Figure S5.9**, the addition of a second network through the formation of an IPN hydrogel (5.0 mM **SQ0SQ-DT**/6.0 mM **PEG$_{2\text{-}2}$**) resulted in a smaller pore size (54 ± 11 µm) compared with the independent PG (6.0 mM **PEG$_{2\text{-}2}$**) (88 ± 37 µm). This observation is consistent with the oscillatory rheology data, where a higher storage modulus of the IPN hydrogel was observed in comparison to the single PG network. When **SQ-DT** was also incorporated into the self-assembled network, the pore size of the DN hydrogel (5.0 mM **SQ10SQ-DT**/6.0 mM **PEG$_{2\text{-}2}$**) was found to be even smaller (15 ± 5 µm). This result supports the formation of additional crosslinks between both networks that reduce the pore size resulting in higher stiffnesses compared to the PG and IPN hydrogels.

The equilibrium water content (EWC) of hydrogels were calculated to further estimate their porosity. This parameter is critical for cell culture applications to offer a highway for the transport of the oxygen, nutrients and other biomolecules to support regular cell function.[28] Overall, all hydrogels tested showed an EWC above 90% (**Figure 5.4A**). The EWC of the independent SG and PG hydrogels were greater than 96%. When the PG networks were mixed into the SG hydrogels, the increased network density resulted in a slightly decreased EWC (95%) for both IPN and DN hydrogels. The relative high EWC value (> 95%) of our IPN and DN hydrogels compared with most of the published DN hydrogel

networks,[12] demonstrated their potential applications for the culture of high water content tissues (e.g., cartilage, muscle tissue).

The degradation kinetics of the hydrogels were further evaluated by calculating the swelling ratio of the various networks at different time points (**Figure 5.4B, C**). The swelling ratio of IPN (5.0 mM **SQ0SQ-DT**/6.0 mM **PEG$_{2\text{-}2}$**) and DN hydrogels with different polymer architectures (e.g., 5.0 mM **SQ10SQ-DT**/6.0 mM **PEG$_{2\text{-}2}$**, 5.0 mM **SQ10SQ-DT**/4.5 mM **PEG$_{2\text{-}4}$**, and 5.0 mM **SQ10SQ-DT**/3.0 mM **PEG$_{4\text{-}4}$**) were stable and remained largely unchanged either maintaining in PBS or cell culture medium (DMEM) at 37 °C for more than 21 days, demonstrating the possibility to use the gel for long-term 3D cell culture, but also for applications where swelling of the hydrogel materials cannot be tolerated.

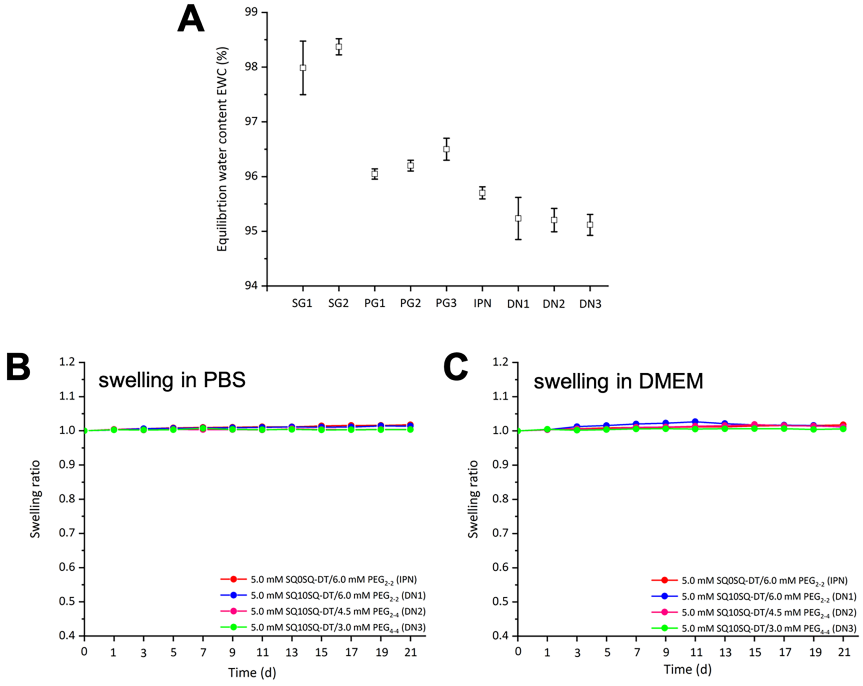

Figure 5.4 (A) Average (N = 3) equilibrium water content (EWC) data for different hydrogel networks formed with exposure to UV light for 3 min. (B) Average (N = 3) swelling ratios of IPN and DN hydrogels formed after 3 min UV irradiation and swelling in PBS (pH 7.4) and DMEM at 37 °C for different time points. Hydrogels: SG1 (5.0 mM **SQ0SQ-DT**); SG2 (5.0 mM **SQ10SQ-DT**); PG1 (6.0 mM **PEG$_{2\text{-}2}$**); PG2 (4.5 mM **PEG$_{2\text{-}4}$**); PG3 (3.0 mM **PEG$_{4\text{-}4}$**); IPN (5.0 mM **SQ0SQ-DT**/6.0 mM **PEG$_{2\text{-}2}$**); DN1 (5.0 mM **SQ10SQ-DT**/6.0 mM **PEG$_{2\text{-}2}$**); DN2 (5.0 mM **SQ10SQ-DT**/4.5 mM **PEG$_{2\text{-}4}$**); DN3 (5.0 mM **SQ10SQ-DT**/3.0 mM **PEG$_{4\text{-}4}$**). UV irradiation was performed with a benchtop LED source (~10 mW/cm^2, 375 nm). Error bars were calculated based on the standard deviation of three independent experiments.

Finally, the potential to couple the RGD peptide or other bioactive proteins throughout our double hydrogel network in a user-defined manner was investigated. For these experiments, a fluorescent RGD peptide **(fluorescein)GK(DT)GGGRGDS**[26] was used to visualize the coupled RGD peptide within the DN hydrogel. The fluorescent RGD-peptide was incorporated in the DN hydrogel (5.0 mM **SQ10SQ-DT**/6.0 mM **$PEG_{2\text{-}2}$**) during its preparation and patterning via two-photon direct laser writing (DLW) was performed. As shown in **Figure S5.10**, an arbitrary cube-like 3D patterns at cell-size relevant length scales was directly written in the hydrogel. Confocal fluorescence microscopy showed a clear difference in the patterned and un-patterned volumes correlated with the variation in the concentration of covalently bound RGD (**Figure S5.10**). Importantly, the ability to perform two-photon laser writing in DN hydrogels opens the door to incorporate bioactive cues at user-defined points in space and time in these mechanically unique materials.

5.3.3 3D cell encapsulation and cell viability study

To examine the suitability of the supramolecular and covalent polymer-based hybrid hydrogels as a synthetic platform *in vitro* for 3D cell culture applications, cell viability of encapsulated NIH 3T3 fibroblasts was first studied in the various hydrogel compositions and concentrations. Using the self-recovery property of DN hydrogels prior to light irradiation, cell-laden hydrogels in 3D were obtained through a simple pipetting process with the cell suspension (see scheme in **Figure 5.1B** and details of the seeding process in supporting information). As shown in **Figure S5.11**, after culture for 24 h, approximately 90% of NIH 3T3 cells remained alive when encapsulated in all the tested IPN and DN hydrogels; for example, hydrogels with different molar percentages of **SQ-DT** (0% or 10%), different total polymer concentrations (3.0 mM **$PEG_{2\text{-}2}$** or 6.0 mM **$PEG_{2\text{-}2}$**) and different polymer architectures (6.0 mM **$PEG_{2\text{-}2}$**, 4.5 mM **$PEG_{2\text{-}4}$**, 3.0 mM **$PEG_{4\text{-}4}$**). Increasing the culture period from day 4 and day 7, did not result in a major difference in cell viability (**Figure S5.11**). These results demonstrate that the various chemistries and processing steps required to prepare the IPN and DN hydrogels, such as the polymers, crosslinking (physical and chemical), and application of light are cytocompatible for extended periods of time with NIH 3T3 cells.

Next, we explored the potential of our DN hydrogel to encapsulate and human primary articular chondrocytes (hPACs) in 3D. To offer the binding sites for cells in the hydrogel matrix and improve the cell-material interactions, the **SQ-**

RGD monomer was introduced into the 5.0 mM **SQ10SQ-DT5SQ-RGD**/6.0 mM **PEG$_{2\text{-}2}$** DN hydrogel. 3D encapsulation of the 3D hPACs was performed in the same manner as for the NIH 3T3 cells above. Cell viability of hPACs within the DN hydrogel was examined for different exposures of the hydrogels to UV irradiation (e.g., 0 min, 1 min and 3 min) with LED (~10 mW/cm^2, 375 nm). As presented in **Figure 5.5**, the cell viability of the encapsulated hPACs after 3 min UV irradiation and 5 days culture was slightly decreased to 80% in comparison to the sample without UV irradiation pointing to the UV dose, or radical nature of the reaction. However, the cell viability was comparable to other photoactivatable hydrogel materials,[29] indicating that our DN hydrogel can be used to support the maintenance of hPACs in 3D *in vitro*.

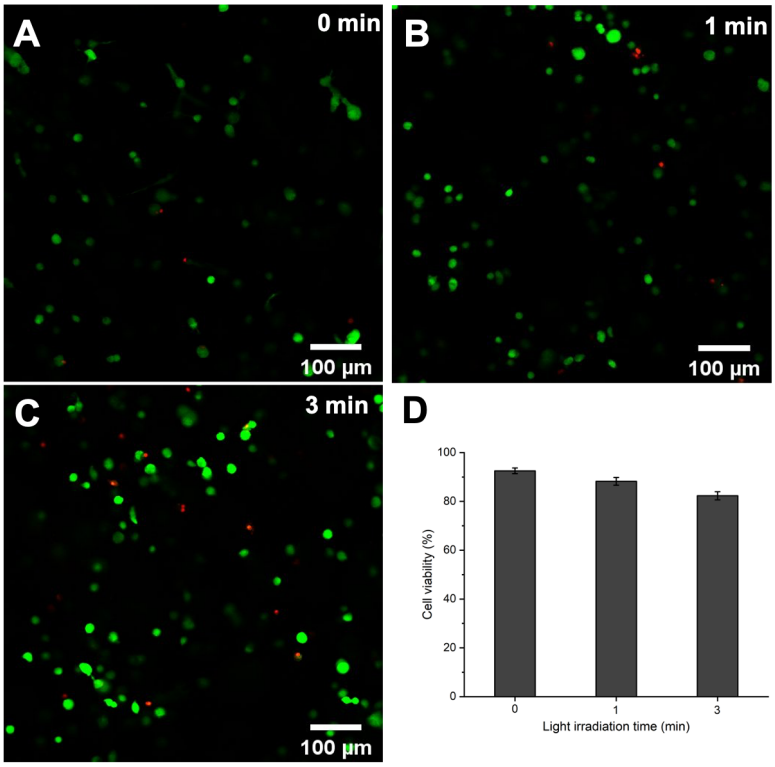

Figure 5.5 Representative confocal microscopy images of calcein AM/PI stainned human primary articular chondrocytes (hPACs) 5 days 3D encapsulated in DN hydrogel (5.0 mM **SQ10SQ-DT5SQ-RGD**/6.0 mM **PEG$_{2\text{-}2}$**) under different exposures to UV irradiation (A: *0 min*, B: *1 min* and C: *3 min*) using a benchtop LED source (~10 mW/cm^2, 375 nm). Scale bar: *100 µm*. Viable cells are stained in green and the dead cells are stained in red. (D) Percentage of viable hPACs within the DN hydrogel after 5 days culture (shown is the average of two independent experiments with error bars for hPACs from different donors).

5.3.4 Extracellular matrix (ECM) formation

In native cartilage *in vivo*, cells generate their own functional extracellular matrix (ECM).[2,3] Therefore, in order for the artificial scaffold to be suitable for cartilage tissue engineering, it should not only be cytocompatible to support the cells survival, but also favor the ECM production. We then explored the deposition of cartilage ECM proteins by encapsulated hPACs and compared this among the varied hydrogel stiffness that were generated by the application of different amounts of UV irradiation (e.g., 0 min, 1 min and 3 min) either in expansion media or in chondrogenic media. To visualize the deposited critical ECM components (sulphated-Glycosaminoglycans (s-GAGs), fibronectin 1, and collagen type II proteins), Alcian blue staining and immunofluorescent staining of the 3D cell-laden hydrogel constructs were also performed. As shown in **Figure 5.6A, C**, ECM was deposited in all tested hydrogels (5.0 mM **SQ10SQ-DT5SQ-RGD**/6.0 mM **PEG_{2}-$_{2}$**) with the maintenance of hPACs in chondrogenic media containing TGF-β1. In comparison to DN hydrogels without UV irradiation, stronger Alcian blue staining was clearly observed within hydrogels exposed to 1 min or 3 min UV irradiation. Likely, this is due to the higher stiffness of hydrogel G' (from 5 Pa for 0 min light to ~ 4000 Pa for 1 min and ~ 7800 Pa for 3 min light) that is consistent with previous results showing that comparable hydrogel stiffness promotes the accumulation of cartilage ECM.[30-32] As a negative control, when the cells were encapsulated in same hydrogel constructs under 0 and 1 min UV irradiation and cultured in the expansion media without TGF-β1, significantly less or no ECM production was observed (**Figure 5.6D, E**), indicating the moderate mechanical hydrogel stiffness and the chondrogenic media are both necessary for triggering ECM deposition by hPACs. Furthermore, immunofluorescent staining of cell-laden DN hydrogels (**Figure 5.6F**), demonstrated the deposition of type II collagen and fibronectin 1 (visualized in red and green, respectively) by encapsulated the hPACs for 5 days in DN hydrogels with 3 min UV irradiation. Together, these results demonstrate that our DN hydrogels enable the preservation of the chondrogenic phenotype of the hPACs and show potential for applications involving articular cartilage engineering.

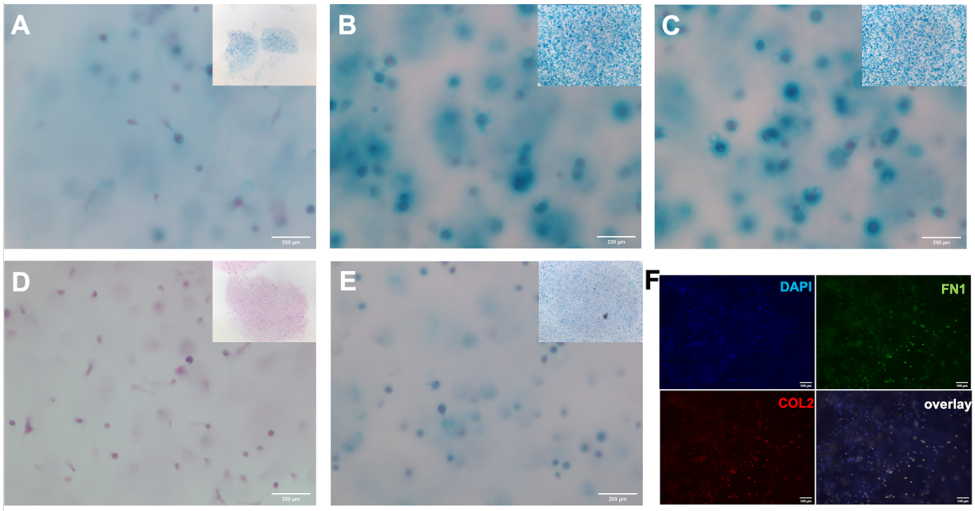

Figure 5.6 After 5 days culture, Alcian blue staining for the s-GAGs with nuclear fast red counterstaining of hPACs in cell-laden DN (5.0 mM **SQ10SQ-DT5SQ-RGD**/6.0 mM **$PEG_{2\text{-}2}$**) scaffolds with varying UV irradiation time and cell culture media: (A) 0 min, (B) 1 min, (C) 3 min UV irradiation and maintained in chondrogenic media containing TGF-β1; (D) 0 min and (E) 1 min UV irradiation and maintained in expansion medium without TGF-β1. (F) Representative immunofluorescent staining images of hPACs cell-laden DN hydrogel 5 days in culture in the chondrogenic media containing TGF-β1 after 3 min UV irradiation (DAPI for blue, FN1 for green, Type II collagen for red and its overlay). UV irradiation was applied through a benchtop LED source (~10 mW/cm^2, 375 nm).

5.4 Conclusions

Here, we report the development of a supramolecular and covalent polymer-based DN hydrogel that is formed through UV light crosslinking. The covalent crosslinks between the supramolecular and polymeric networks were established through ring opening of the cyclic 1,2-dithiolane (DT) motif. More specifically, UV irradiation of the networks results in both the simultaneous reaction between the DT units of the monomers in the supramolecular networks or the DT/NB units with the covalent polymer network in one-pot reaction with the aid of a photoinitiator and light source. Moreover, their mechanical, self-recovering and compressible properties can easily be tuned by varying the molar percent of **SQ-DT**, total polymer concentration and polymer architectures with UV light. Additionally, the stiffness and bioactive RGD peptide can be spatiotemporally introduced into the double network under similar UV irradiation conditions. Their cytocompatible response of NIH 3T3 and hPACs in the DN hydrogel materials under the experimental conditions, show the chemical reactions for crosslinks and also the light source used are suitable *in vitro* experiments in 3D. Importantly, the increased matrix deposition by the encapsulated hPACs in DN hydrogels with increasing stiffness opens the door for their application *in vitro* for articular cartilage engineering.

5.5 References

(1) Kim, I. L.; Mauck, R. L.; Burdick, J. A. *Biomaterials* **2011**, *32* (34), 8771-8782.
(2) Chen, F. H.; Rousche, K. T.; Tuan, R. S. *Nat. Clin. Pract. Rheumatol.* **2006**, *2* (7), 373-382.
(3) Sophia Fox, A. J.; Bedi, A.; Rodeo, S. A. *Sports Health* **2009**, *1* (6), 461-468.
(4) Vega, S. L.; Kwon, M. Y.; Burdick, J. A. *Eur. Cells Mater.* **2017**, *33*, 59-75.
(5) Armiento, A. R.; Stoddart, M. J.; Alini, M.; Eglin, D. *Acta Biomater.* **2018**, *65*, 1-20.
(6) Freedman, B. R.; Mooney, D. J. *Adv. Mater.* **2019**, *31* (19), e1806695.
(7) Anderson, D. E.; Johnstone, B. *Front. Bioeng. Biotechnol.* **2017**, *5*, 76.
(8) Chen, Q.; Chen, H.; Zhu, L.; Zheng, J. *J. Mater. Chem.* **2015**, *3* (18), 3654-3676.
(9) Haque, M. A.; Kurokawa, T.; Gong, J. P. *Polymer* **2012**, *53* (9), 1805-1822.
(10) Zhao, X. *Soft Matter* **2014**, *10* (5), 672-687.
(11) Gu, Z.; Huang, K.; Luo, Y.; Zhang, L.; Kuang, T.; Chen, Z.; Liao, G. *Wiley Interdiscip Rev. Nanomed. Nanobiotechnol.* **2018**, *10* (6), e1520.
(12) Means, A. K.; Grunlan, M. A. *ACS Macro Lett.* **2019**, *8* (6), 705-713.
(13) Sun, W.; Xue, B.; Li, Y.; Qin, M.; Wu, J.; Lu, K.; Wu, J.; Cao, Y.; Jiang, Q.; Wang, W. *Adv. Funct. Mater.* **2016**, *26* (48), 9044-9052.
(14) Rodell, C. B.; Dusaj, N. N.; Highley, C. B.; Burdick, J. A. *Adv. Mater.* **2016**, *28* (38), 8419-8424.
(15) Wang, H.; Zhu, D.; Paul, A.; Cai, L.; Enejder, A.; Yang, F.; Heilshorn, S. C. *Adv. Funct. Mater.* **2017**, *27* (28), 1605609.
(16) Li, L.; Zhang, K.; Wang, T.; Wang, P.; Xue, B.; Cao, Y.; Zhu, L.; Jiang, Q. *Mater. Des.* **2020**, *189*, 108492.
(17) Hilderbrand, A. M.; Ford, E. M.; Guo, C.; Sloppy, J. D.; Kloxin, A. M. *Biomater. Sci.* **2020**, *8* (5), 1256-1269.
(18) Li, C.; Rowland, M. J.; Shao, Y.; Cao, T.; Chen, C.; Jia, H.; Zhou, X.; Yang, Z.; Scherman, O. A.; Liu, D. *Adv. Mater.* **2015**, *27* (21), 3298-3304.
(19) Zhang, H. J.; Sun, T. L.; Zhang, A. K.; Ikura, Y.; Nakajima, T.; Nonoyama, T.; Kurokawa, T.; Ito, O.; Ishitobi, H.; Gong, J. P. *Adv. Mater.* **2016**, *28* (24), 4884-4890.
(20) Tamesue, S.; Noguchi, S.; Kimura, Y.; Endo, T. *ACS Appl. Mater. Interfaces* **2018**, *10* (32), 27381-27390.
(21) Loebel, C.; Ayoub, A.; Galarraga, J. H.; Kossover, O.; Simaan-Yameen, H.; Seliktar, D.; Burdick, J. A. *J. Mater. Chem. B* **2019**, *7* (10), 1753-1760.
(22) Ouyang, L.; Highley, C. B.; Rodell, C. B.; Sun, W.; Burdick, J. A. *ACS Biomater. Sci. Eng.* **2016**, *2* (10), 1743-1751.
(23) Wang, L. L.; Highley, C. B.; Yeh, Y. C.; Galarraga, J. H.; Uman, S.; Burdick, J. A. *J. Biomed. Mater. Res. A* **2018**, *106* (4), 865-875.
(24) Margulis, K.; Zhang, X.; Joubert, L. M.; Bruening, K.; Tassone, C. J.; Zare, R. N.; Waymouth, R. M. *Angew. Chem. Int. Ed.* **2017**, *56* (51), 16357-16362.
(25) Song, L.; Zhang, B.; Gao, G.; Xiao, C.; Li, G. *Eur. Polym. J.* **2019**, *115*, 346-355.

(26) Tong, C.; Wondergem, J. A. J.; Heinrich, D.; Kieltyka, R. E. *ACS Macro Lett.* **2020**, *9* (6), 882-888.
(27) Scheutz, G. M.; Rowell, J. L.; Ellison, S. T.; Garrison, J. B.; Angelini, T. E.; Sumerlin, B. S. *Macromolecules* **2020**, *53* (10), 4038-4046.
(28) Perez-Madrigal, M. M.; Shaw, J. E.; Arno, M. C.; Hoyland, J. A.; Richardson, S. M.; Dove, A. P. *Biomater. Sci.* **2020**, *8* (1), 405-412.
(29) Pahoff, S.; Meinert, C.; Bas, O.; Nguyen, L.; Klein, T. J.; Hutmacher, D. W. *J. Mater. Chem. B* **2019**, *7* (10), 1761-1772.
(30) Lee, H. P.; Gu, L.; Mooney, D. J.; Levenston, M. E.; Chaudhuri, O. *Nat. Mater.* **2017**, *16* (12), 1243-1251.
(31) Tan, Y.; Huang, H.; Ayers, D. C.; Song, J. *ACS Cent. Sci.* **2018**, *4* (8), 971-981.
(32) Loebel, C.; Kwon, M. Y.; Wang, C.; Han, L.; Mauck, R. L.; Burdick, J. A. *Adv. Funct. Mater.* **2020**, *30* (44), 1909802.

5.6 Supporting Information

5.6.1 Materials and instruments

Poly (ethylene glycol) (Mw 6 kDa) was obtained from Fluka, and 4 arm-PEG-OH (MW 10 kDa) from Jenkem Technology. All other chemicals and reagents for synthesis were purchased from Sigma Aldrich and directly used without further purification. Deuterated solvent for NMR experiments were obtained from Eurisotop. Water was deionized before use. Dulbecco's phosphate buffered saline (DPBS) was purchased from Sigma Aldrich. Dulbecco's modified Eagle medium (DMEM) was received from Gibco, Life Technologies. Fetal bovine serum (FBS) was achieved from Biowest. The antibiotics penicillin and streptomycin were purchased from Gibco. Collagenase Type I was obtained from Worthington Biochemical Corporation. Calcein AM, Propidium Iodide (PI), Alcian Blue 8-GX, Nuclear fast red-aluminum sulfate, and normal goat serum were received from Sigma Aldrich. The goat anti-mouse Alexa Fluor 647 and goat anti-rabbit Alexa Fluor 488 were obtained from Abcam. µ-Slide 15 well plates were purchased from Ibidi. Polydimethylsiloxane (PDMS) (Sylgard 184 Silicon Elastomer Kit, Dow Corning), silicon wafers and fluorosilane (1H,1H,2H,2H-perfluorooctyltrichlorosilane) were purchased from VWR chemicals, Siegert Wafers and Sigma-Aldrich, respectively. Monomers **SQ**, **SQ-DT**, **SQ-RGD**, fluorescent RGD peptide (**(Fluorescein)GK(DT)GGGRGDS**), **PEGdiNB** (6 kDa), and **PEGdiDT** (6 kDa) were synthesized as previously described in **chapter 2-4**. Purification of supramolecular monomers (**SQ**, **SQ-DT**, and **SQ-RGD**) and fluorescent RGD peptide were achieved on a Grace Reveleris X1 flash chromatography system with a C18 column, following by RP-HPLC on a Vydac C18 reverse-phase column with UV detection. ^{1}H-NMR and ^{13}C-NMR spectra were collected at room temperature on a Bruker DMX-400 (400 MHz). LC-MS data were recorded on a Finnigan Surveyor HPLC system with Gemini C18 column (50 × 4.60 mm, UV detection: 200-600 nm) and also a Finnigan LCQ Advantage Max mass spectrometer with ESI. A solvent gradient of 10-90% of CH_3CN-H_2O with 0.1% TFA through 13.5 min was used as the mobile phase. Oscillatory rheology experiments were performed on a Discovery Hybrid Rheometer (DHR-2, TA Instruments) using a parallel plate geometry (20 mm diameter) with a UV curing accessory at room temperature. The UV light source connected to the rheology was obtained from the Excelitas Omnicure S2000 system (λ = 320-500 nm, primary peak: 365 nm) through a light guide (5 mm diameter). Scanning electron micrographs (SEM) were

collected on a JSM-7600F microscope (JEOL) under a high vacuum with an acceleration voltage of 2.0 kV. 3D photopatterning was performed on a Photonic Professional GT (Nanoscribe, Germany) with a 20x air objective (Zeiss, Germany). The photo-patterned hydrogels were imaged on a Nikon Eclipse Ti microscope equipped with a Yokogawa confocal spinning disk unit operated at 10,000 rpm (Nikon) with a 20x objective. Cell viability studies of the cells encapsulated in the hydrogels were imaged on a Zeiss LSM 710 confocal laser scanning microscope equipped with a Zeiss 10x objective. The 3D cell-laden hydrogels for immunocytochemical staining were imaged in Leica SP5.

5.6.2 Synthetic procedures

Synthesis of PEG4NB (10 kDa)

PEG4NB was synthesized according to a previously published protocol.[1] 5-Norbornene-2-carboxcylic acid (1.42 g, 10.26 mmol) was stirred in dichloromethane (DCM, 10 mL) in a round bottom flask (100 mL) at room temperature. Dicyclohexylcarbodiimide (DCC) (1.06 g, 5.13 mmol) was added slowly yielding a white precipitate byproduct, and the reaction was further stirred for another 30 min at room temperature. In a separate round bottom flask (100 mL), 4-arm PEG-OH (Mw 10 kDa) (4.27 g, 0.43 mmol) was dissolved in DCM (15 mL), together with pyridine (690 µL, 8.55 mmol) and 4-dimethylaminopyridine (DMAP) (0.10 g, 0.86 mmol). The two flasks were then combined and the reaction was stirred overnight at room temperature. The reaction mixture was first filtered to remove any white solid byproduct from the DCC reagent, and further concentrated using a stream of air prior to being precipitated in cold diethyl ether. Finally, the mixture was washed, and re-dissolved in DCM. The precipitation steps above were repeated for three cycles. The end product obtained was then re-dissolved in deionized water, dialyzed for three days (changing the deionized water two times per day) and lyophilized overnight to obtain a white solid.

Yield: 3.54 g, 83%. ^{1}H-NMR (400 MHz, $CDCl_3$) 6.17-5.90 (m, 2H), 4.22-4.15 (m, 2H), 3.85-3.25 (m, 224H).

The degree of norbornene functionalization was confirmed using ^{1}H-NMR spectroscopy (400 MHz, $CDCl_3$). The extent of norbornene substitution was calculated by the ratio of integrals obtained for alkene protons on norbornene (6.17-5.90 ppm, 1.58H) to that of actual value for complete conversion (6.17-5.90

ppm, 2H) which was found to be 80%. The protons (3.85-3.25 ppm, 224H) were used for calibration.

Synthesis of PEG4DT (10 kDa)

1,2-Dithiolane (DT) was synthesized according to a previously published protocol.[2] DT (1.25 g, 7.64 mmol) was dissolved in DCM (10 mL) in a round bottom flask (100 mL) and DCC (0.79 g, 3.82 mmol) was added. The formation of a yellow precipitate by-product dicyclohexylurea was observed and the obtained reaction mixture was stirred for 30 min at room temperature. In a separate round bottom flask (100 mL), 4-arm PEG-OH (Mw 10 kDa) (3.18 g, 0.32 mmol) was dissolved in DCM (12 mL), and then pyridine (514 µL, 6.36 mmol) and DMAP (0.078 g, 0.64 mmol) were added. The two flasks were then combined together and the reaction mixture was stirred overnight at room temperature. The reaction mixture was filtered to remove the yellow solid byproduct, and concentrated by a stream of air before being precipitated in cold diethyl ether, washed, and re-dissolved in DCM. The above precipitation step was repeated for three cycles. The obtained end product was further re-dissolved in deionized water, dialyzed for three days (changing deionized water two times per day) and lyophilized overnight to obtain a solid.

Yield: 2.8 g, 88%. ^{1}H-NMR (400 MHz, $CDCl_3$) 4.30-4.27 (m, 2H), 3.81-3.39 (m, 226H), 2.93-2.90 (m, 2H), 1.47 (s, 3H).

The degree of dithiolane functionalization was confirmed using ^{1}H-NMR spectroscopy (400 MHz, $CDCl_3$). The extent of dithiolane substitution was calculated by the ratio of integrals obtained for -CH_2 from dithiolane motif (2.93-2.90 ppm, 1.66H) to that of actual value for complete conversion (2.93-2.90 ppm, 2H) which was found to be around 80%. The protons (3.81-3.39 ppm, 226H) were used for calibration.

5.6.3 Hydrogel preparation

Preparation of supramolecular hydrogels (SG)

The preparation of the supramolecular hydrogels (SG), e.g., **SQxSQ-DT** (where x is the molar percentage of **SQ-DT** divided by the total concentration), was executed according to the protocol described in **chapter 3**. Briefly, **SQ** and **SQ-DT** stock solutions (10.0 mM) were separately prepared by dissolving the **SQ** and **SQ-DT**

powders in dimethyl sulfoxide (DMSO) with 2 min of vortexing. To acquire **SQxSQ-DT** hydrogels with various total monomer concentrations or different **SQ-DT** molar percentages (x), a pre-determined volume of the DMSO stock solutions of **SQ** and **SQ-DT** were pipetted into a glass vial (2 mL) followed by 30 s of gentle vortexing to obtain homogeneous solutions. The DMSO was removed using a stream of N_2 overnight. Then, the required volume of PBS (pH 7.4) was added to obtain the desired concentration, and sonication in an ultrasonic water bath was performed for 30 min to 2 h (~4 °C with ice). The sonication time necessary depends on the monomer concentration and the power of the sonication bath used. The clear solutions obtained were then incubated at 37 °C in an oven for 15 min to trigger gel formation. Transparent hydrogels of **SQxSQ-DT** were further equilibrated at room temperature overnight prior to any other measurements.

Preparation of PEG-based hydrogels (PG) containing DT and NB end-groups

The preparation of PEG-based polymeric hydrogels $\mathbf{PEG_{m\text{-}n}}$ (m and n: the architecture of dithiolane (DT) and norbornene (NB)-functionalized PEG precursors) followed a previously published protocol.[3] Here, the preparation of the $\mathbf{PEG_{2\text{-}2}}$ (containing **PEGdiDT** (6 kDa), **PEGdiNB** (6 kDa) and **LAP**) hydrogel will be discussed as an example. First, stock solutions of **PEGdiDT**, **PEGdiNB** and **LAP** were prepared separately by dissolving each component in PBS (pH 7.4) in a vial (2 mL) with 30 s of vortexing. Then, **PEGdiDT** (70 µL), **PEGdiNB** (70 µL) and **LAP** (10 µL) stock solutions were pipetted into a new vial (2 mL) followed by another 30 s of vortexing to obtain a homogeneous precursor solution (150 µL). The transparent polymeric hydrogel $\mathbf{PEG_{2\text{-}2}}$ was formed after UV light irradiation for 3-10 min either through the Excelitas Omnicure S2000 system (~10 mW/cm^2, λ = 320-500 nm, primary peak: 365 nm) or a benchtop LED (~10 mW/cm^2, 375 nm). The volume ratio of **PEGdiDT**, **PEGdiNB** and **LAP** was always kept at 7:7:1. The same procedure was used to prepare the other polymeric hydrogel systems, for example, $\mathbf{PEG_{2\text{-}4}}$ (containing **PEGdiDT** (6 kDa), **PEG4NB** (10 kDa) and **LAP**), and $\mathbf{PEG_{4\text{-}4}}$ (containing **PEG4NB** (10 kDa), **PEG4DT** (10 kDa) and **LAP**).

Preparation of hybrid hydrogels (IPN and DN)

To obtain the IPN (e.g., **SQ0SQ-DT**/$\mathbf{PEG_{2\text{-}2}}$) and DN (**SQ10SQ-DT**/$\mathbf{PEG_{2\text{-}2}}$) hydrogels, a pre-determined volume of the PEG stock solutions dissolved in deionized water (**PEGdiDT** (70 µL) and **PEGdiNB** (70 µL)) were pipetted into a new vial (2 mL) and

gently pipetted up and down (10 times) to obtain homogeneous solutions (140 µL). The **PEGdiDT**/**PEGdiNB** solution was lyophilized overnight to obtain a solid. Aliquots of PBS (20 µL) and **LAP** stock solutions (10 µL) were added to re-dissolve the above **PEGdiDT**/**PEGdiNB** solids to obtain the stock solution **PEG$_{2\text{-}2}$** (30 µL). Then, the supramolecular stock solution **SQ0SQ-DT** or **SQ10SQ-DT** (120 µL) after sonication in an ice bath (to prevent gelation) was directly pipetted into the polymeric stock solution **PEG$_{2\text{-}2}$** (30 µL), followed by gentle up and down pipetting (10 times) to achieve a homogenous solution containing both types of polymers (150 µL). The samples were then equilibrated in a 37 °C oven for 15 min to trigger supramolecular gel formation, followed by being left to stand overnight at room temperature prior to light irradiation. Finally, the IPN and DN hydrogels were formed after UV irradiation for 3-10 min either through the Excelitas Omnicure S2000 system (~10 mW/cm^2, λ = 320-500 nm, primary peak: 365 nm) or a benchtop LED (~10 mW/cm^2, 375 nm). To prepare the hybrid supramolecular and covalent hydrogels, the volume ratio of the SG and PG was always maintained at 4:1. The preparation of all other hybrid hydrogels followed the same procedure as mentioned above.

5.6.4 Gel inversion experiments

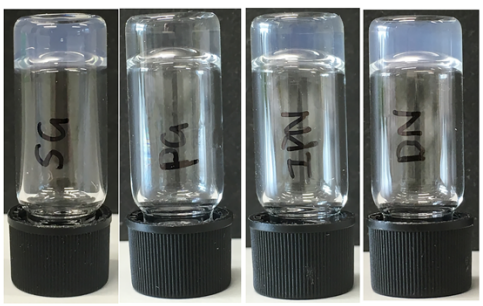

Figure S5.1 Gel inversion experiments of hydrogels after 3 min UV irradiation using a benchtop LED source (~10 mW/cm2, 375 nm) at room temperature: SG (5.0 mM **SQ10SQ-DT**); PG (6.0 mM **PEG$_{2\text{-}2}$**); IPN (5.0 mM **SQ0SQ-DT**/6.0 mM **PEG$_{2\text{-}2}$**); and DN (5.0 mM **SQ10SQ-DT**/6.0 mM **PEG$_{2\text{-}2}$**).

5.6.5 Oscillatory rheology

The pre-prepared hydrogels (SG, IPN, DN) (110 µL) and pre-gelated PG solutions (104 µL) were gently pipetted on to a PMMA plate (20 mm diameter). The gap between the geometry and the plate was set at 300 mm. The samples were irradiated under an Excelitas Omnicure S2000 system (~10.0 mW/cm^2, λ = 320-

500 nm, primary peak: 365 nm) using a light guide with 5 mm diameter. The UV light was turned on after data was recorded for 600 s. To characterize the rheological properties, oscillatory time sweeps (f = 1.0 Hz, γ = 0.05%), frequency sweeps from 0.01 to 10 Hz (γ = 0.05%), and strain sweeps from 0.01 to 1000% (f = 1.0 Hz) were collected. The self-recovery properties were measured using a step-strain experiment. After the above strain experiment, a time-dependent recovery measurement was applied at low strain (γ = 0.05%) for 300 s. Once the storage modulus (G') reached its plateau, a high strain (γ = 500%) was applied for another 300 s. The application of high- and low strain in an alternating fashion was repeated for two cycles. The recovery rate of hydrogel systems was calculated by collecting the storage moduli before (G_0') and after (G_t') strain was applied. The recovery rate (%) was determined as following: recovery rate (%) = (G_t'/G_0')*100%.

The compression experiments were performed on the rheometer using an axial force test with maximum force (50 N). The prepared samples (400 µL) were loaded on to the PMMA plate (20 mm diameter) and a gap (1200 µm) was used. The samples were first irradiated with UV light using an Excelitas Omnicure S2000 system (~10.0 mW/cm^2, λ = 320-500 nm, primary peak: 365 nm) for 10 min to reach a plateau in storage modulus. Then, an axial experiment was set up compressing the sample to 50% of its initial height (600 µm gap), with a constant linear deformation rate (10 µm/s). The normal stress was plotted versus the cauchy strain (or engineering strain, the change in gap percentage as measured with respect to its initial setting) to examine the compression properties for different hydrogel systems.

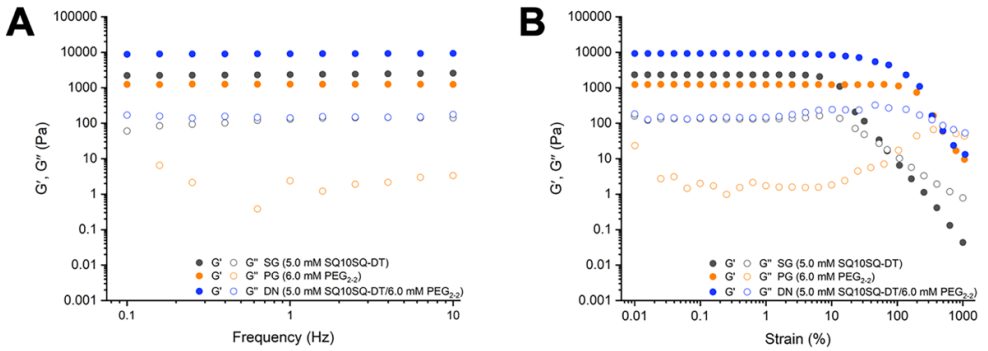

Figure S5.2 Averaged (N = 3) (A) frequency (0.1-10 Hz) and (B) strain (0.01-1000%) sweeps of hydrogels with various compositions after 10 min UV irradiation (~10 mW/cm^2, λ = 320-500 nm, primary peak: 365 nm) at room temperature: SG (5.0 mM **SQ10SQ-DT**), PG (6.0 mM **PEG$_{2\text{-}2}$**) and DN (5.0 mM **SQ10SQ-DT**/6.0 mM **PEG$_{2\text{-}2}$**). The frequency sweep experiment was performed at a fixed strain (γ = 0.05%) and the strain experiment was collected at constant frequency (f = 1.0 Hz).

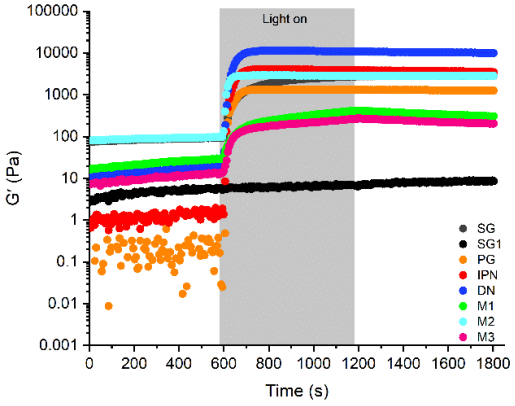

Figure S5.3 Averaged (N = 3) time sweep experiment of various hydrogels after 10 min UV irradiation (~10 mW/cm^2, λ = 320-500 nm, primary peak: 365 nm) measured at a fixed frequency (f = 1.0 Hz) and strain (γ = 0.05%) at room temperature: (1) SG (5.0 mM **SQ10SQ-DT**); (2) SG1 (5.0 mM **SQ0SQ-DT**) (2) PG (6.0 mM **PEG$_{2\text{-}2}$**); (3) IPN (5.0 mM **SQ0SQ-DT**/6.0 mM **PEG$_{2\text{-}2}$**); (4) DN (5.0 mM **SQ10SQ-DT**/6.0 mM **PEG$_{2\text{-}2}$**); (5) M1 (5.0 mM **SQ10SQ-DT**/6.0 mM **PEG$_{2\text{-}2}$**/no **LAP**); (6) M2 (5.0 mM **SQ10SQ-DT**/3.0 mM **PEGdiNB**/1.0 mM **LAP**); and (7) M3 (5.0 mM **SQ10SQ-DT**/3.0 mM **PEGdiDT**/1.0 mM **LAP**). The shaded area shows when the UV light was applied.

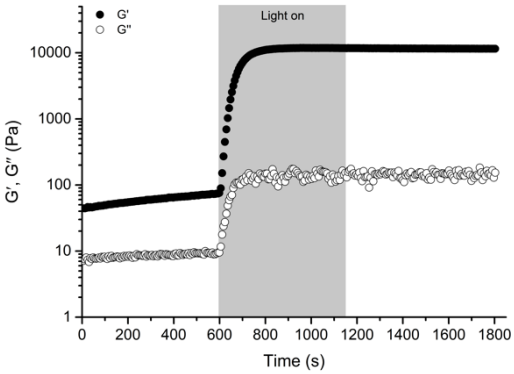

Figure S5.4 Averaged (N = 2) time sweep experiment of DN hydrogel (10.0 mM **SQ5SQ-DT**/6.0 mM **$PEG_{2\text{-}2}$**) after 10 min UV irradiation (~10 mW/cm^2, λ = 320-500 nm, primary peak: 365 nm) measured at a fixed frequency (f = 1.0 Hz) and strain (γ = 0.05%) at room temperature. The shaded area shows when the UV light was applied.

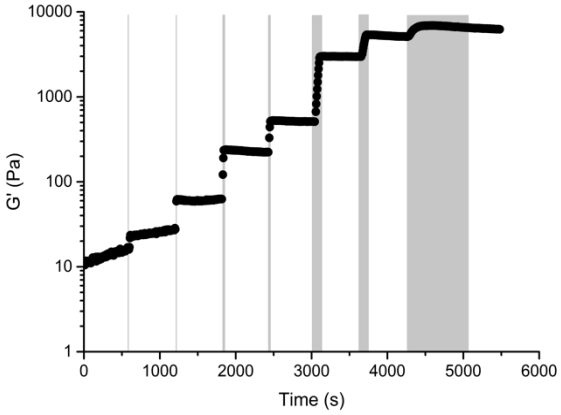

Figure S5.5 The averaged (N = 2) time sweep experiment of DN hydrogel (5.0 mM **SQ10SQ-DT**/6.0 mM **$PEG_{2\text{-}2}$**) through step UV light irradiation (10 mW/cm^2, wavelength: 320-500 nm, primary peak: 365 nm). The data was collected at a fixed frequency (f = 1.0 Hz) and strain (γ = 0.05%) at room temperature. The shaded area shows when the UV light was applied.

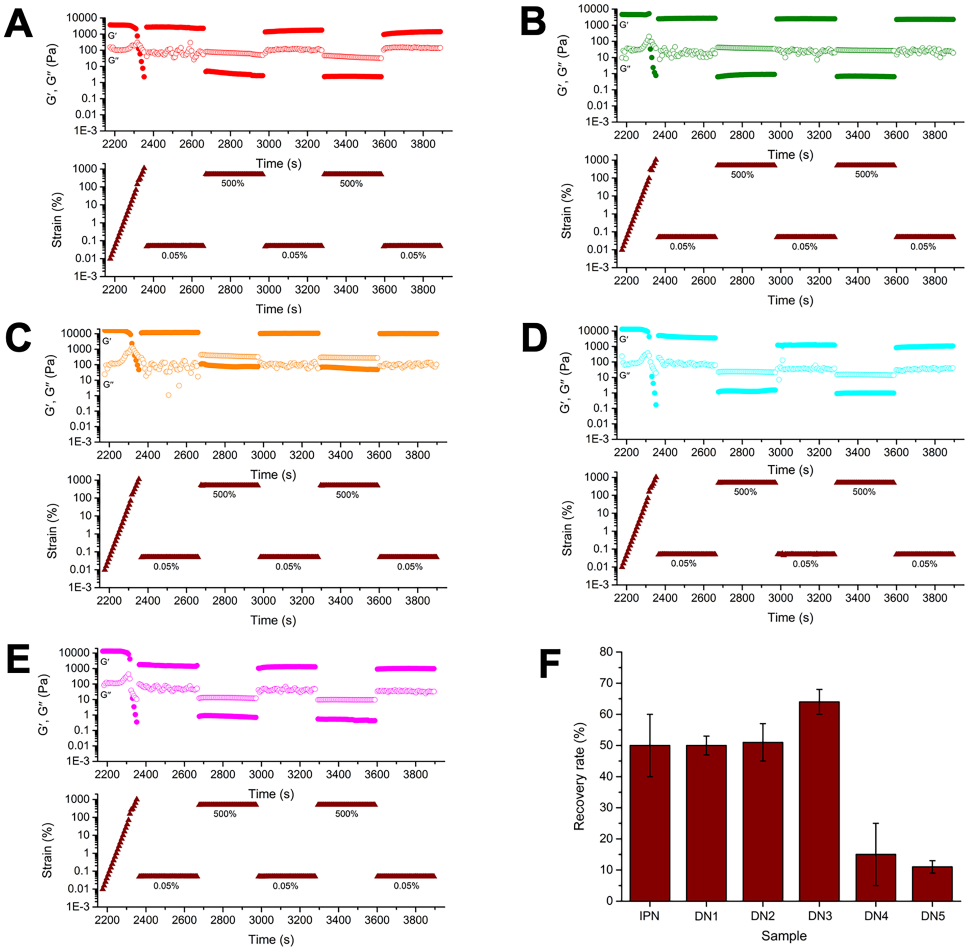

Figure S5.6 Averaged (N = 3) strain experiment and step-strain measurement of various IPN and DN hydrogels after 10 min UV irradiation at a constant of frequency (f = 1.0 Hz): (A) IPN (5.0 mM **SQ0SQ-DT**/6.0 mM **PEG$_{2\text{-}2}$**); (B) DN1 (5.0 mM **SQ10SQ-DT**/3.0 mM **PEG$_{2\text{-}2}$**); (C) DN3 (5.0 mM **SQ10SQ-DT**/12.0 mM **PEG$_{2\text{-}2}$**); (D) DN4 (5.0 mM **SQ10SQ-DT**/4.5 mM **PEG$_{2\text{-}4}$**) and (E) DN5 (5.0 mM **SQ10SQ-DT**/3.0 mM **PEG$_{4\text{-}4}$**). (F) The averaged (N = 3) storage recovery rate of various IPN and DN hydrogels. DN2: 5.0 mM **SQ10SQ-DT**/6.0 mM **PEG$_{2\text{-}2}$**. For all measurements, UV irradiation condition: ~10 mW/cm^2, wavelength: 320-500 nm, primary peak: 365 nm. Error bars were calculated according the average of independent repeat measurements (N = 3).

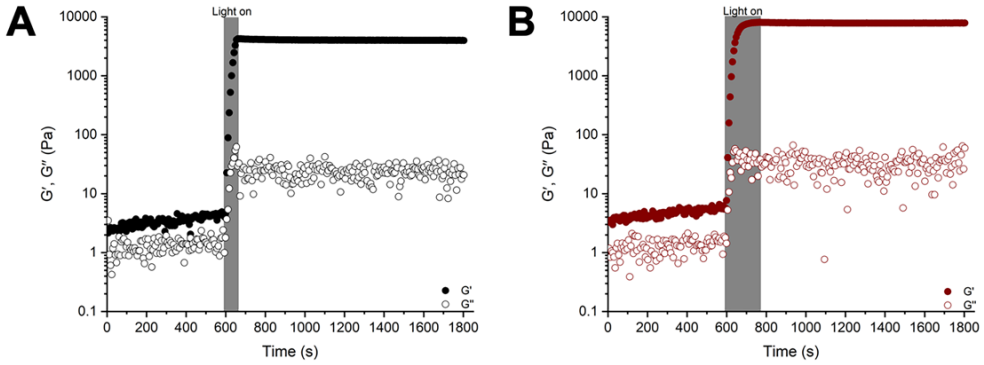

Figure S5.7 Averaged (N = 2) time sweep experiment of DN hydrogel (5.0 mM **SQ10SQ-DT5SQ-RGD**/6.0 mM **PEG$_{2\text{-}2}$**) under different UV irradiation time (~10 mW/cm^2, λ = 320-500 nm, primary peak: 365 nm) measured at a fixed frequency (f = 1.0 Hz) and strain (γ = 0.05%) at room temperature: (A) 1 min and (B) 3 min. The shaded area shows when the UV light was applied.

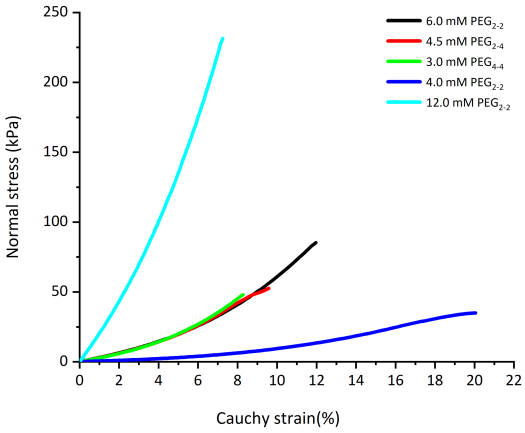

Figure S5.8 The averaged (N = 3) normal stress-cauchy strain curves of different PG hydrogels after 10 min UV irradiation (~10 mW/cm^2, wavelength: 320-500 nm, primary peak: 365 nm): (1) 4.0 mM **PEG$_{2\text{-}2}$**; (2) 6.0 mM **PEG$_{2\text{-}2}$**; (3) 12.0 mM **PEG$_{2\text{-}2}$**; (4) 4.5 mM **PEG$_{2\text{-}4}$**; (5) 3.0 mM **PEG$_{4\text{-}4}$**.

Table S5.1 Gelation behaviors and plateau storage moduli (G') of systems (SG, PG, IPN and DN) with different hydrogel compositions (e.g., supramolecular monomer concentration, **SQ-DT** molar percent in **SQ10SQ-DT**, polymer concentration, and polymer architectures) and also the various UV light parameters (λ = 320-500 nm, primary peak: 365 nm). Averaged G' values are presented (N ≥ 3).

System	Sample name	Composition (mM)		Light irradiation time (min)	Pre-UV light Storage moduli G' (Pa)	Post-UV light Storage moduli G' (Pa)
		SQxSQ-DT (SG)	**PEG_{m-n}** (PG)			
SG	**SQ0SQ-DT**	5.0	-	10	5 ± 1	8 ± 1
	SQ1SQ-DT	5.0	-	10	9 ± 3	196 ±114
	SQ5SQ-DT	5.0	-	10	44 ± 10	1392 ± 541
	SQ10SQ-DT	5.0	-	10	91 ± 15	2816 ± 519
PG	**PEG_{2-2}**	-	3.0	10	S	VS
		-	4.0	10	S	177 ± 32
		-	6.0	10	S	1284 ± 56
	PEG_{2-4}	-	4.5	10	S	1267 ± 102
	PEG_{4-4}	-	3.0	10	S	1240 ± 230
IPN	**SQ0SQ-DT/PEG_{2-2}**	5.0	3.0	10	VS	473 ± 118
		5.0	3.0	3	VS	239 ± 90
		5.0	4.0	10	VS	1093 ± 283
		5.0	6.0	10	VS	3704 ± 243
		5.0	6.0	3	VS	4193 ± 2351
DN	**SQ1SQ-DT/PEG_{2-2}**	5.0	6.0	10	VS	7833 ± 583
	SQ5SQ-DT/PEG_{2-2}	5.0	6.0	10	5 ± 1	10250 ± 627
		10.0	6.0	10	71 ± 2	11606 ± 553
	SQ10SQ-DT/PEG_{2-2}	5.0	3.0	10	10 ± 8	3028 ± 129
		5.0	3.0	3	22 ± 9	2182 ± 350
		5.0	4.0	10	15 ± 12	4994 ± 370
		5.0	6.0	10	16 ± 7	10391 ± 541
		5.0	6.0	3	10 ± 5	9371 ± 213
		5.0	8.0	10	10 ± 10	11815 ± 351
		5.0	12.0	10	4 ± 2	17307 ± 4273
		5.0	16.0	10	VS	21072 ± 5071
	SQ10SQ-DT/PEG_{2-4}	5.0	6.0	10	7 ± 3	13688 ± 1338
	SQ10SQ-DT/PEG_{4-4}	5.0	6.0	10	13 ± 1	12253 ± 2387

S: Solution; VS: Viscous solution.

5.6.6 Scanning electron microscopy (SEM)

The hydrogels (300 μL): (1) PG (6.0 mM **PEG_{2-2}**); (2) IPN (5.0 mM **SQ0SQ-DT**/6.0 mM **PEG_{2-2}**) and (3) DN (5.0 mM **SQ10SQ-DT**/6.0 mM **PEG_{2-2}**) were prepared as discussed above and irradiated with UV light for 3 min using a benchtop LED source (~10.0 mW/cm^2, 375 nm). The hydrogels were subsequently freeze-dried overnight and then, fractured after briefly dipping the solids in liquid nitrogen using tweezers. The fractured pieces were directly applied to two-sided adhesive tape, placed on an aluminum stub and coated for 2 min by a thin layer of gold (under vacuum) before imaging.

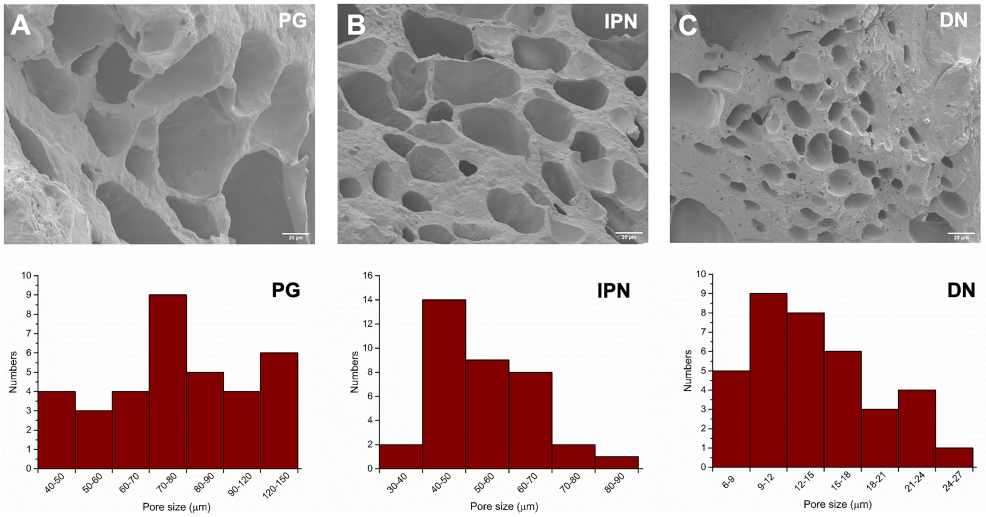

Figure S5.9 SEM images of various hydrogel systems (A) PG: 6.0 mM **$PEG_{2\text{-}2}$**; (B) IPN: 5.0 mM **SQ0SQ-DT**/6.0 mM **$PEG_{2\text{-}2}$**; (C)DN: 5.0 mM **SQ10SQ-DT**/6.0 mM **$PEG_{2\text{-}2}$** and also their relative distribution of pore size. The pore size was measured from the SEM images using the Image J software. Scale bar: *20 μm*.

5.6.7 Equilibrium water content (EWC)

All samples (SG, PG, IPN, DN) (150 μL) were prepared in a glass vial (2.0 mL) and irradiated with UV light using a benchtop LED (~10.0 mW/cm^2, 375 nm) for 3 min. To determine the equilibrium water content (EWC), hydrogels were first allowed to swell in PBS (pH 7.4, 600 μL) at 37 °C in an incubator for 24 h to reach equilibrium swelling. Prior to measuring the hydrogel weight (W_s), the PBS was removed with a micropipette and blotted with a soft tissue paper to remove any excess. The hydrogels were then lyophilized overnight and the weight was recorded (W_d). For all samples, three independent replicate experiments were performed. The EWC for each hydrogel was calculated using: EWC (%) = (W_s-W_d)/W_s*100%.

5.6.8 Swelling and degradation assays

The swelling ratios of the hydrogels were determined according to a previously published method.[4] Individual samples (150 μL) were first prepared in a glass vial (2.0 mL) and irradiated with UV light for 3 min using a benchtop LED (~10 mW/cm^2, 375 nm). The original gel weight (W_0) of each hydrogel prior to swelling was measured. Subsequently, each hydrogel was covered either with PBS (pH 7.4) or cell culture medium (DMEM) (600 μL), and then incubated at 37 °C. The weight

(W_t) of all hydrogels was then collected at pre-determined time points, after complete removal of PBS or DMEM from the surface. The fresh PBS and DMEM were changed every two days during swelling. Three independent replicates were performed for each hydrogel condition. The swelling ratio was determined as W_t/W_0.

5.6.9 Two-photon crosslinking of fluorescent RGD peptide through direct laser writing

Two-photon crosslinking of the fluorescent RGD peptide was performed by direct laser writing (DLW) following a previous procedure in **chapter 3**.[3] The 3D structures were designed in Autodesk Inventor and converted to a stereolithographic file format (STL). Then, the STL files were imported into DeScribe (Nanoscribe GmbH) to obtain a suitable mesh for DLW. The pre-made hybrid hydrogel mixture (5.0 mM **SQ10SQ-DT**/6.0 mM **$PEG_{2\text{-}2}$**) containing the fluorescent RGD peptide (**(FL)GK(DT)GGGRGDS**) (10 μM) was pipetted into custom cut PDMS inserts placed on glass microscope coverslips (#1.5, 30 mm, Thermo Fisher Scientific). The sample was exposed to a laser (Ti-Sapphire, 780 nm, 20 mW maximum at sample surface) with a 20x Air objective. In the x, y-directions the DLW mesh was scanned by the laser through galvanic mirrors, and then stitched, slice-by-slice, in the z-direction with a piezo stage. Scanning speed of 250 μm/s together with a power scaling of 1.0 were set. All DLW procedures were performed under yellow light (λ = 577-597 nm) to avoid spontaneous cross-linking during the writing process. After two-photon crosslinking, the samples were washed with PBS (5 times) to remove the uncoupled fluorescent RGD peptide and covered with PBS to avoid drying.

The two-photon patterned sample was imaged on a Nikon Eclipse Ti microscope with a 20x objective. The attached fluorescein was excited using light (488 nm, 0.2 mW) from a solid-state diode laser (Coherent) supported in an Agilent MLC4 unit (Agilent Technologies). Images were captured using an exposure time of 300 ms by an Andor iXon Ultra 897 High Speed EM-CCD camera (Andro Technology). For 3D image reconstruction, acquired fluorescent images were background corrected to visualize hydrogel sections that underwent crosslinking.

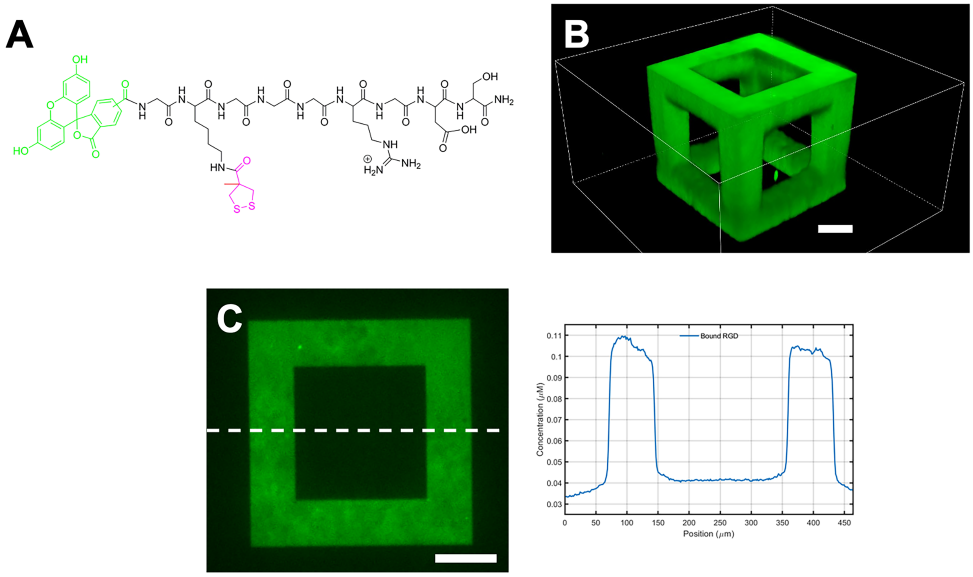

Figure S5.10 (A) Chemical structure of fluorescent RGD peptide (**(fluorescein)GK(DT)GGGRGDS**). (B) Representative images using confocal microscopy of the bound fluorescent RGD peptide throughout the DN hydrogel (5.0 mM **SQ10SQ-DT**/6.0 mM **$PEG_{2\text{-}2}$**) obtained via 3D direct-laser writing (DLW). (C) Raw 2D confocal fluorescence image of bounded fluorescent RGD peptide (*left*) and a graph of the measured concentration versus the position along the dashed line (*right*), highlighting the difference of the patterned and un-patterned area. Scale bar: *100 μm.*

5.6.10 Cell culture

NIH 3T3 cell culture. NIH 3T3 cells were cultured and maintained in DMEM medium containing 10% fetal bovine serum (FBS), penicillin (100 units/mL) and streptomycin (100 μg/mL) in an incubator at 37 °C at a 5% CO_2 atmosphere.

Human primary articular chondrocytes (hPACs) culture. Collection and expansion of human primary articular chondrocytes (hPACs) from the ongoing Research Arthritis and Articular Cartilage (RAAK) study was performed as earlier described.[5] In short, within 2 hours following joint replacement surgery of osteoarthritis patients, cartilage of the preserved region of the joint was sampled in DMEM (high glucose) supplemented with 10% FBS, antibiotics penicillin (100 units/mL) and streptomycin (100 μg/mL) and collagenase Type I (2 mg/mL); and were incubated overnight at 37 °C incubator with a humidified 95% and 5% CO_2 atmosphere. Isolated chondrocytes were expanded for 2 passages in DMEM supplemented with 10% FBS, antibiotics (100 units/mL penicillin and 100 μg/mL streptomycin) and FGF-2 (0.5 ng/mL) prior to encapsulation into the hydrogel materials.

5.6.11 3D cell encapsulation

3D cell encapsulation of NIH 3T3 cells in varied hydrogel compositions (e.g., 5.0 mM **SQ0SQ-DT**/6.0 mM **$PEG_{2\text{-}2}$**; 5.0 mM **SQ10SQ-DT**/3.0 mM **$PEG_{2\text{-}2}$**; 5.0 mM **SQ10SQ-DT**/6.0 mM **$PEG_{2\text{-}2}$**; 5.0 mM **SQ10SQ-DT**/4.5 mM **$PEG_{2\text{-}4}$**; and 5.0 mM **SQ10SQ-DT**/3.0 mM **$PEG_{4\text{-}4}$**) was carried out according to the following protocol: a single cell suspension of NIH 3T3 cells was obtained by trypsinization, centrifugation and resuspension in DMEM. The obtained cell suspension (15 µL, ~15 × 10^6 cells/mL) was mixed with the hydrogels (135 µL) by gently pipetting up and down (~10 times) to obtain a homogeneous cell-gel mixture. The volume ratio of the hydrogel to the cell suspension was always kept at 9:1. Then the obtained cell-hydrogel mixture was gently pipetted into a µ-Slide 15 well plate (12 µL) and directly irradiated with UV light (3 min) using a benchtop LED source (~10 mW/cm^2, 375 nm) to provide the cell-laden hydrogels in 3D. Cell culture media (48 µL) was carefully layered on top of the hydrogels and cultured in an incubator at 37 °C with a 5% CO_2 atmosphere. The cell media was refreshed daily during the experiment.

3D cell encapsulation of hPACs cells in DN hydrogel, namely, 5.0 mM **SQ10SQ-DT5SQ-RGD**/6.0 mM **$PEG_{2\text{-}2}$**, containing the RGD based bioactive cues (**SQ-RGD**), was explored. The hPACs suspension at a density of 5 x 10^6 cells/mL (counted with NucleoCounter® NC-200™) was encapsulated in DN hydrogel following the same procedure as NIH 3T3 cells above. Different UV irradiation times (0 min, 1 min, and 3 min) were applied using a benchtop LED (~10 mW/cm^2, 375 nm) to the 3D cell-laden hydrogel mixtures. Then, 3D constructs were covered with DMEM expansion medium or in chondrogenic differentiation medium (DMEM high glucose supplemented with Ascorbate (50 µg/mL), Dexamethasone (0.1 µM), L-proline (40 µg/mL), Sodium pyruvate (100 µg/mL), ITS-plus, antibiotics, and TGF-β1 (10 ng/mL), and cultured under standard conditions (37 °C with a 5% CO_2 atmosphere). Cell culture media were refreshed daily during the experiment.

5.6.12 Cell viability study

The LIVE/DEAD (calcein AM/propidium iodide (PI)) assay was used to study cell viability after encapsulation of the cells (e.g., NIH 3T3 and hPACs) within the hydrogel.

For the LIVE/DEAD study of NIH 3T3 cells, the mixed staining solutions of calcein AM (2.0 µM) and PI (1.5 µM) were prepared by diluting pre-prepared stock

solutions of calcein AM (2.5 mM in DMSO) and PI (1.5 mM in PBS) with PBS (pH 7.4). At pre-determined time points (e.g., day 1, 4 and 7), the medium was removed from the top of the hydrogel, and washed with PBS (2 x 48 µL). This was followed by covering the hydrogel with the staining solution (48 µL) for 30 min at 37 °C. Then, the staining solution was removed from the top of hydrogel, and further washed with PBS (2 x 48 µL). An additional volume of PBS (48 µL) was pipetted on top of the hydrogel to prevent drying during imaging.

LIVE/DEAD staining of hPACs was performed after 5 days of culture within hydrogels. Medium from the constructs was first removed and incubated with PBS for 15 min at 37°C. After washing, PBS was removed and replaced by calcein AM solution in DMEM (0.25 µM) at 37°C for 20 min. Subsequently, calcein AM was removed, and Propidium Iodide (PI) solution in DMEM (30 µM) was added for 5 min at room temperature. Finally, the PI staining solution was removed and the cell-laden construct was washed with PBS (3 x 48 µL) for 15 min at 37°C. The construct was covered with fresh PBS before imaging.

Fluorescent Z-stack images were obtained on a Zeiss LSM 710 confocal laser scanning microscope using a 10x objective and a 488 nm for excitation of calcein AM and a 532 nm laser for excitation of the PI dye. The Image J software package was used to process the collected raw images and count cell viability.

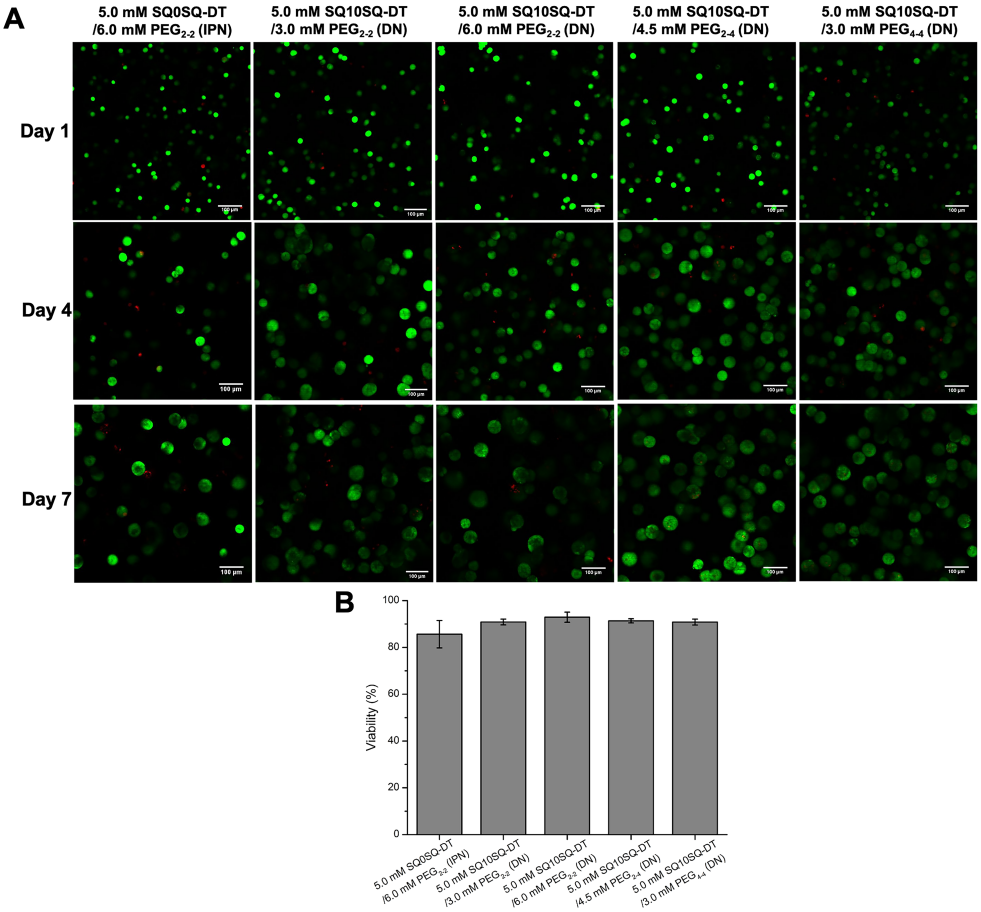

Figure S5.11 NIH 3T3 cells were encapsulated in various IPN and DN hydrogels in 3D with different compositions and concentrations of components in the double network gels after 3 min UV irradiation using a benchtop LED (~10 mW/cm², 375 nm): (1) 5.0 mM **SQ0SQ-DT**/6.0 mM **PEG$_{2\text{-}2}$**; (2) 5.0 mM **SQ10SQ-DT**/3.0 mM **PEG$_{2\text{-}2}$**; (3) 5.0 mM **SQ10SQ-DT**/6.0 mM **PEG$_{2\text{-}2}$**; (4) 5.0 mM **SQ10SQ-DT**/4.5 mM **PEG$_{2\text{-}4}$**; and (5) 5.0 mM **SQ10SQ-DT**/3.0 mM **PEG$_{4\text{-}4}$**. (A) Confocal microscopy images of calcein AM/PI stainned NIH 3T3 cells after encapsulating in hydrogels at different culture time points (e.g., day 1, day 4 and day 7). Scale bar: *100 μm*. Green for viable cells and red for dead cells. (B) Averaged (N = 3) cell viabilities of NIH 3T3 cells after 24 h culture in the various gels.

5.6.13 Alcian blue staining

After 5 days of culture within the hydrogels, hPACs were first fixed with 4% formaldehyde at room temperature for 15 min. Subsequently, constructs were washed 3 times with PBS and incubated with 0.1N HCl for 10 min. To detect sulphated-glycosaminoglycans (s-GAGs), constructs were incubated with 1% solution of Alcian Blue 8-GX in 0.1N HCl for 1 h and washed 3 times with 0.1N HCl

to remove excess Alcian Blue, followed by washing 3 times with milliQ water. Cell nuclei was counterstained with 0.1% nuclear fast red in 5% aluminum sulfate for 10 min and washed 3 times with MilliQ water before imaging with bright field microscopy.

5.6.14 Immunocytochemical staining

To visualize collagen type 2 and fibronectin 1, after 5 days of culture, the constructs were first fixed with 4% paraformaldehyde at room temperature for 15 min. After washing the constructs 3 times with PBS, cells were permeabilized using 0.5% Triton X-100 solution in PBS at room temperature for 10 min. Constructs were washed 3 times with PBS at room temperature for 5 min. Antigen retrieval was accomplished with Proteinase K treatment (5 µg/mL) for 10 min at 37°C, followed by Hyaluronidase treatment (5 mg/mL) for 30 min at 37°C. After 3 times washing with PBS for 5 min and blocking of non-specific binding with 5% normal goat serum in PBS, constructs were incubated overnight at 4°C with the antibodies. Then the constructs were washed 3 times with PBS and incubated at room temperature for 1 hour with secondary antibodies (goat anti-mouse Alexa Fluor 647 and goat anti-rabbit Alexa Fluor 488) in block solution (5% normal goat serum in PBS). After 3 times washing PBS, constructs were covered with VECTASHIELD Antifade Mounting Medium with DAPI prior to imaging.

5.6.15 References

(1) Fairbanks, B. D.; Schwartz, M. P.; Halevi, A. E.; Nuttelman, C. R.; Bowman, C. N.; Anseth, K. S. *Adv. Mater.* **2009**, *21* (48), 5005-5010.
(2) Yu, H.; Wang, Y.; Yang, H.; Peng, K.; Zhang, X. *J. Mater. Chem. B* **2017**, *5* (22), 4121-4127.
(3) Tong, C.; Wondergem, J. A. J.; Heinrich, D.; Kieltyka, R. E. *ACS Macro Lett.* **2020**, *9* (6), 882-888.
(4) Yang, F.; Wang, J.; Cao, L.; Chen, R.; Tang, L.; Liu, C. *J. Mater. Chem. B* **2014**, *2* (3), 295-304.
(5) Bomer, N.; den Hollander, W.; Ramos, Y. F.; Bos, S. D.; van der Breggen, R.; Lakenberg, N.; Pepers, B. A.; van Eeden, A. E.; Darvishan, A.; Tobi, E. W.; Duijnisveld, B. J.; van den Akker, E. B.; Heijmans, B. T.; van Roon-Mom, W. M.; Verbeek, F. J.; van Osch, G. J.; Nelissen, R. G.; Slagboom, P. E.; Meulenbelt, I. *Ann. Rheum. Dis.* **2015**, *74* (8), 1571-1579.